

## Clutter Invariant ATR

Dmitri Bitouk, Michael I. Miller, *Sr. Member, IEEE*,  
and Laurent Younes

**Abstract**—One of the central problems in Automated Target Recognition is to accommodate the infinite variety of clutter in real military environments. The principle focus of our paper is on the construction of metric spaces where the metric measures the distance between objects of interest invariant to the infinite variety of clutter. Such metrics are formulated using second-order random field models. Our results indicate that this approach significantly improves detection/classification rates of targets in clutter.

**Index Terms**—Riemannian metrics, deformable templates, Automated Target Recognition (ATR).

### 1 INTRODUCTION

ONE of the central problems in Automated Target Recognition is to accommodate the infinite variety of clutter in real military environments. In model-based approaches, identification/classification rates are largely determined by the accuracy of models used to represent real-world scenes. In heavy cluttered environments, it is impractical to explicitly represent each of the objects in the scene by a deterministic 3D model, whereas applying a low-dimensional statistical description of clutter may improve ATR performance in clutter. The modeling of clutter can be approached from the point of view of empirical statistics. Similar approaches have been successfully carried out under the context of modeling object signatures using principal component analysis [1], [2], [3]. Unquestionably, the main challenge to model-based methods is to acquire the pose and identification of targets while at the same time “seeing through” the confounding clutter.

In this paper, we construct robust deformable templates, which allow us to accommodate both variations of the pose of objects and photometric variations associated with natural clutter. To perform object detection and identification, we build robust deformable templates into a metric space structure, computing a metric distance between robust deformable templates and observed images.

The variability of target type and pose can be accommodated using a rigid template approach, defining for every target type a template with a group of rigid motions representing geometric variations. In a continuous setting, the set of images  $\mathcal{I}$  is defined as a space of functions on the background space  $X$ ,  $I : X \rightarrow V$ , with  $V$  the value space. In this paper, we consider  $X \subset \mathbb{R}^k$ ,  $k = 2, 3$ , and  $V = \mathbb{R}$ . The group of geometric transformations  $G$  acts on the background space  $X$  according to  $g \in G : x \in X \rightarrow g \circ x \in X$ . The group action of  $G$  on the image space  $\mathcal{I}$  is defined by its action of the background space  $g \in G : I \in \mathcal{I} \rightarrow I \circ g \in \mathcal{I}$ . The rigid template corresponds to the orbit  $G.I_{temp}$  under the group action  $G$  of one selected and fixed image  $I_{temp}$

$$G.I_{temp} = \{I \in \mathcal{I} : I = I_{temp} \circ g, g \in G\}. \quad (1)$$

For the purposes of automated target recognition, images  $I_{temp}$  correspond to the targets.

- The authors are with the Center for Imaging Science, Whiting School of Engineering, The Johns Hopkins University, 3400 North Charles Street, Baltimore, MD 21218. E-mail: {dimas, mim, younes}@cis.jhu.edu.

Manuscript received 08 Jan. 2003; revised 29 June 2004; accepted 1 Nov. 2004; published online 11 Mar. 2005.

Recommended for acceptance by R. Chellappa.

For information on obtaining reprints of this article, please send e-mail to: tpami@computer.org, and reference IEEECS Log Number 118108.

Variability in observed images is not solely associated with geometric transformations, which define the pose of targets, but also the presence of clutter and many other factors such as lighting variations, object surface properties, and texture variations. Thus, the variability in the observed imagery consists of geometric as well as so-called photometric transformations. The deformable template is made robust by expanding it from the purely geometric transformations of pose to include the photometric variabilities. The group of photometric variations is modeled as a Hilbert space  $H \subseteq L_2$ . Since not all of the elements of  $L_2$  correspond to observable images, the space of photometric variations  $H$ , constructed via basis expansion  $\{\psi_n\}$ , is bound to be a very small subset of  $L_2$ . Its action on the space of images  $\mathcal{I}$  is additive

$$h = \sum_n I_n \psi_n \in H : I \in \mathcal{I} \rightarrow I + \sum_n I_n \psi_n \in \mathcal{I}. \quad (2)$$

The group  $A = G \otimes H$ , consisting of both geometric and photometric variations, is defined as a semidirect product of groups  $G$  and  $H$  with elements  $\{(g, I) : g \in G, I \in H\}$ . The robust deformable template  $A.I_{temp}$  becomes the orbit under the action of the group  $A$

$$A.I_{temp} = \left\{ I \in \mathcal{I} : I = \left( I_{temp} + \sum_n I_n \psi_n \right) \circ g \right\}. \quad (3)$$

For the clutter problem, it appears that a complementary approach should be taken, modeling the background rather than the targets themselves.

The metric-space formulation is based on computing a deformation which transforms one image into the other. The metric distance is related to the energy required to perform such a deformation. In the template matching settings, one computes the metric distance between an observed image  $I_D$  and the template  $I_{temp}$ , which represents the object of interest (a target) present in the observed image. For the purpose of target discrimination, the metric distance should be robust with respect to both geometric transformations of the templates and the infinite photometric variety in the observed images associated with natural clutter. In this paper, we make the orbit into a metric space constructing the metric to be robust to the action of the group of geometric and photometric changes by modeling the covariance structure of the empirical statistics of the cluttered backgrounds and building that into the norm of the metric determining the geodesics in the orbit.

### 2 METRIC SPACE FORMULATION OF DEFORMABLE TEMPLATES

Construction of a metric distance on  $\mathcal{I}$ , which takes into account the action of  $G$ , usually requires using a variational approach on the product space  $G \times \mathcal{I}$  in which the metric would be defined through a geodesic distance. The principle of this construction relies on defining the energy of paths on  $G \times \mathcal{I}$  with subsequent computation of the distance by minimizing these energies as described in [4]. A differentiable path on  $G \times \mathcal{I}$  is a continuous function  $(g_t, I_t) : [0; 1] \rightarrow G \times \mathcal{I}$  for which the time derivative

$$\left( \frac{dg_t}{dt}, \frac{dI_t}{dt} \right)$$

is defined for all  $t \in [0; 1]$ . Given a collection of functional norms  $\mathcal{N}_G$  and  $\mathcal{N}_{\mathcal{I}}$ , the associated energy of the path  $(g_t, I_t)$  is

$$E(g_t, I_t) = \int_0^1 \mathcal{N}_G \left( \frac{\partial g_t}{\partial t} \circ g_t^{-1} \right)^2 dt + \int_0^1 \mathcal{N}_{\mathcal{I}} \left( \frac{\partial I_t}{\partial t} \circ g_t^{-1} \right)^2 dt. \quad (4)$$

Then, the distance  $d(I^{(0)}, I^{(1)})$  on  $\mathcal{I}$  is defined through the infimum energy over all the paths  $g_t$  starting at the identity,  $g_0 = id$ , and all the paths  $I_t$ , which take  $I^{(0)}$  to  $I^{(1)} \circ g_1$

$$d(I^{(0)}, I^{(1)}) = \inf_{\substack{g_t : g_0 = id, \\ I_t : I_0 = I^{(0)}, I_1 = I^{(1)} \circ g_1}} \sqrt{E(g_t, I_t)}, \quad (5)$$

where  $id$  is the identity transformation.

In (4), there are two penalty terms for the deformation, which takes  $I^{(0)}$  to  $I^{(1)}$ . The first integral penalizes transformations in the background space associated with the group  $G$ , and the second one penalizes photometric deformations. In general, the choice of the norms  $\mathcal{N}_G$  and  $\mathcal{N}_{\mathcal{I}}$  depends on the application. In this work, the group  $G$  associated with the pose of the objects of interest is considered to be the group of rigid motions,  $G = SO(k) \otimes \mathbb{R}^k$ , which consist of all possible rotations and translation in  $k$ -dimensional space. The natural requirement would be to set the penalty, which is due to the rigid motions of the objects, to zero,  $\mathcal{N}_G(\cdot) \equiv 0$ . On the other hand, another desired property of the metric distance, in this case, is robustness with respect to photometric variations in the observed images associated with natural clutter. This property can be achieved by designing norms  $\mathcal{N}_{\mathcal{I}}$  using statistical models of natural clutter.

## 2.1 Image Norms Induced by Covariance of Clutter

Markov Random Field models are especially attractive to model statistical properties of clutter in real-world scenes [5]. However, the complexity can be greatly reduced by using stationary Gaussian Markov Random Field [6], [7] models while still capturing important statistical properties of natural clutter. In these models, clutter is characterized by the Toeplitz covariance  $K(x, 0), x \in \Omega \subset \mathbb{R}^k$ . Although it has been pointed out by many authors that natural images are strongly non-Gaussian [8], [9], second-order statistics capture important information about spatial correlation between pixels. To induce the norm for photometric variability and, therefore, the geodesic structure of the deformable template, we craft the norm to correspond to the covariance structure of the empirical statistical world of clutter. Such methodology is similar in spirit to the adaptive matched filtering approaches to ATR [10], [11].

Assuming that the covariance kernel  $K(x, y)$  to be Hilbert-Schmidt  $\iint K^2(x, y) dx dy < \infty$ , the Hilbert-Schmidt theorem implies that there exists a complete orthonormal sequence of eigenfunctions  $\{\psi_n(x)\}$  with corresponding eigenvalues  $\{\lambda_n\}$  such that  $\int K(x, y) \psi_n(y) dy = \lambda_n \psi_n(x)$ . Let us define a Hilbert space  $H \subseteq L_2$  according to  $H = \{f \in L_2 : \|f\|_H^2 < \infty\}$ , with the norm  $\|\cdot\|_H$ , induced by the kernel  $K(x, y)$ ,

$$\|f\|_H^2 = \sum_n \frac{|\langle f, \psi_n \rangle_{L_2}|^2}{\lambda_n}. \quad (6)$$

Now, consider an element  $g$  in the group of rigid motions  $G = SO(k) \otimes \mathbb{R}^k$ . The kernel  $K(g \circ x, g \circ y)$  is also Hilbert-Schmidt and induces a corresponding Hilbert space  $g.H$ . The following lemma establishes the connection between the norms  $\|\cdot\|_H$  and  $\|\cdot\|_{g.H}$ :

**Lemma 1.** For any  $f \in g.H$ ,

$$\|f\|_{g.H} = \|f \circ g^{-1}\|_H. \quad (7)$$

**Proof.** Let  $\{\tilde{\psi}_n\}$  be a complete orthonormal sequence of eigenfunctions of  $K(g \circ x, g \circ y)$  with corresponding eigenvalues  $\{\tilde{\lambda}_n\}$

$$\int K(g \circ x, g \circ y) \tilde{\psi}_n(y) dy = \tilde{\lambda}_n \tilde{\psi}_n(x). \quad (8)$$

A simple substitution of variables  $x \rightarrow g^{-1} \circ x, y \rightarrow g^{-1} \circ y$  in the integral implies  $\tilde{\psi}_n = \psi_n \circ g, \tilde{\lambda}_n = \lambda_n$ , giving

$$\|f\|_{g.H}^2 = \sum_n \frac{|\langle f, \tilde{\psi}_n \circ g \rangle_{L_2}|^2}{\lambda_n} = \sum_n \frac{|\langle f \circ g^{-1}, \psi_n \rangle_{L_2}|^2}{\lambda_n} = \|f \circ g^{-1}\|_H^2. \quad (9)$$

□

## 2.2 Metrics Induced by Empirical Covariance

Now, we design a metric distance on the set of images  $\mathcal{I}$  under the action of the group of rigid motions defined as  $g \circ x = Rx + b$ , where  $R \in SO(k), b \in \mathbb{R}^k$ . Following the basic framework of this section, we set the penalty term for geometric transformations  $G$  to zero,  $\mathcal{N}_G \equiv 0$  and associate the covariance norms  $\|\cdot\|_{g.H}$ , defined in the previous section, with the functional norm  $\mathcal{N}_{\mathcal{I}}$ . Then, the energy of the path  $E(g_t, I_t)$  will be defined through the norm  $\left\| \frac{\partial I_t}{\partial t} \circ g_t^{-1} \right\|_{g_t^{-1}.H}^2$  involving the covariance. The measure of similarity between two images  $d(I^{(0)}, I^{(1)})$  is defined as a metric distance,  $d : \mathcal{I} \times \mathcal{I} \rightarrow [0; +\infty)$  according to

$$d(I^{(0)}, I^{(1)}) = \inf_{g_t, I_t, g_0 = id : I_0 = I^{(0)}, I_1 = I^{(1)} \circ g_1} \sqrt{\int_0^1 \left\| \frac{dI_t}{dt} \circ g_t^{-1} \right\|_{g_t^{-1}.H}^2 dt}. \quad (10)$$

The function  $d(I^{(0)}, I^{(1)})$  is defined via an equivalent optimization problem.

**Lemma 2.** Defining  $J_t = I_t \circ g_t^{-1}$ ,

$$d(I^{(0)}, I^{(1)}) = \inf_{\substack{\Omega(t), \beta(t) : \Omega_0 = 0, \beta_0 = 0 \\ J_t : J_0 = I^{(0)}, J_1 = I^{(1)}}} \sqrt{\int_0^1 \left\| \frac{dJ_t}{dt} + \left\langle \frac{\partial J_t}{\partial x}, \Omega(t)x + \beta(t) \right\rangle_{\mathbb{R}^k} \right\|_{g_t^{-1}.H}^2 dt}, \quad (11)$$

where  $\Omega(t)$  is a skew-symmetric matrix defined by

$$\frac{dR(t)}{dt} = \Omega(t)R(t), \quad \beta(t) = \frac{db(t)}{dt} - \Omega(t)b(t). \quad (12)$$

**Proof.** Computing the derivative of  $I_t$  yields

$$\frac{dI_t}{dt} = \frac{\partial J_t}{\partial t} \circ g_t + \left\langle \frac{\partial J_t}{\partial x} \circ g(t), \Omega(t)(R(t)x + b(t)) + \beta(t) \right\rangle_{\mathbb{R}^k}, \quad (13)$$

$$\frac{dI_t}{dt} \circ g_t^{-1} = \frac{\partial J_t}{\partial t} + \left\langle \frac{\partial J_t}{\partial x}, \Omega(t)x + \beta(t) \right\rangle_{\mathbb{R}^k}. \quad (14)$$

Noting the fact that  $g_t$  is uniquely identified by the velocities  $\Omega(t)$  and  $\beta(t)$  and vice versa, one concludes that taking infimum over  $g_t$  is equivalent to the infimum over  $\Omega(t)$  and  $\beta(t)$ . □

We remark that the distance associated with the variational problem for  $d(I^{(0)}, I^{(1)})$  connects to the statistical setting of the maximum likelihood estimation problem given by the equality of

$$d^2(I^{(0)}, I^{(1)}) = \inf_{g_1} \|I^{(0)} - I^{(1)} \circ g_1\|_H^2. \quad (15)$$

To see this, apply the Lemma 1 of  $\|\cdot\|_{g_t^{-1}.H}$  giving

$$\begin{aligned} d^2(I^{(0)}, I^{(1)}) &= \inf_{g_t, I_t, g_0 = id : I_0 = I^{(0)}, I_1 = I^{(1)} \circ g_1} \int_0^1 \left\| \frac{dI_t}{dt} \circ g_t^{-1} \right\|_{g_t^{-1}.H}^2 dt \quad (16) \end{aligned}$$

$$= \inf_{g_t, I_t, g_0 = id : I_0 = I^{(0)}, I_1 = I^{(1)} \circ g_1} \int_0^1 \left\| \frac{dI_t}{dt} \right\|_H^2 dt. \quad (17)$$

This implies that  $I_t$  is a linear interpolation of its boundary conditions

$$I_t = (1-t)I^{(0)} + tI^{(1)} \circ g_1 \quad (18)$$

with

$$\frac{dI_t}{dt} = I^{(1)} \circ g_1 - I^{(0)}$$

and substituting back into the definition of  $d(I^{(0)}, I^{(1)})$  gives the equivalence.

In the statistical framework, the variational problem for  $d(I^{(0)}, I^{(1)})$  corresponds to the imaging model  $I^{(0)} = I^{(1)} \circ g_1 + W$ , where  $I^{(0)}$  is an observation of the template  $I^{(1)}$  transformed by the rigid motion  $g_1$  and corrupted by an additive stationary second-order random field  $W$ , which covariance is specified by the kernel  $K(x, 0)$ . Note that the metric distance  $d(I^{(0)}, I^{(1)})$  is the closest distance in the sense of covariance-induced norm between the observed image and the corresponding template under all possible geometric transformations.

### 2.3 Invariance Properties

For an arbitrary covariance  $K(x, 0)$ , a measure of similarity  $d(I^{(0)}, I^{(1)})$ , defined by (10), is not a metric distance on  $\mathcal{I}$  since it is not symmetric and does not satisfy the triangular inequality. In this section, the conditions are provided under which  $d(I^{(0)}, I^{(1)})$  is a metric distance. The following theorem establishes the connection between invariance properties of  $d(I^{(0)}, I^{(1)})$  and  $K(x, y)$ :

**Theorem 1.** *Suppose for all  $h \in G = SO(k) \otimes \mathbb{R}^k$   $K(h \circ x, h \circ y) = K(x, y)$ . Then, for any  $h \in G = SO(k) \otimes \mathbb{R}^k$ , the function  $d(I^{(0)}, I^{(1)})$  is invariant under the action of  $G$ , i.e.,*

$$d^2(I^{(0)} \circ h, I^{(1)} \circ h) = d^2(I^{(0)}, I^{(1)}). \quad (19)$$

Given a Toeplitz covariance  $K(x, 0)$  which is invariant under the action of  $SO(k)$ ,

$$K(r \circ x, 0) = K(x, 0), \quad \forall r \in SO(k), \quad (20)$$

the function  $d : \mathcal{I} \times \mathcal{I} \rightarrow \mathbb{R}^+$ , defined by (10), is a metric distance on  $\mathcal{I}$ .

**Proof.** Using (15) yields

$$d^2(I^{(0)} \circ h, I^{(1)} \circ h) = \inf_g \left\| I^{(0)} \circ h - (I^{(1)} \circ h) \circ g \right\|_H^2 = \inf_g \sum_n \frac{|\langle I^{(0)} \circ h - (I^{(1)} \circ h) \circ g, \psi_n \rangle_{L_2}|^2}{\lambda_n}. \quad (21)$$

The inner product in (21) is rewritten making a change of variables  $x \rightarrow h^{-1} \circ x$  inside both the inner products giving

$$\langle I^{(0)} \circ h, \psi_n \rangle_{L_2} = \langle I^{(0)}, \psi_n \circ h^{-1} \rangle_{L_2}, \quad (22)$$

$$\left\langle (I^{(1)} \circ h) \circ g, \psi_n \right\rangle_{L_2} = \left\langle I^{(1)} \circ (h \circ g \circ h^{-1}), \psi_n \circ h^{-1} \right\rangle_{L_2}. \quad (23)$$

The distance  $d^2(I^{(0)} \circ h, I^{(1)} \circ h)$  takes the form

$$d^2(I^{(0)} \circ h, I^{(1)} \circ h) = \inf_g \sum_n \frac{|\langle I^{(0)} - I^{(1)} \circ (h \circ g \circ h^{-1}), \psi_n \circ h^{-1} \rangle_{L_2}|^2}{\lambda_n}, \quad (24)$$

and, from (9),

$$d^2(I^{(0)} \circ h, I^{(1)} \circ h) = \inf_g \left\| I^{(0)} - I^{(1)} \circ (h \circ g \circ h^{-1}) \right\|_{h^{-1}H}^2. \quad (25)$$

The invariance of the covariance kernel under the action  $G$ ,  $K(h \circ x, h \circ y) = K(x, y)$ , implies that, for any  $h \in G$ , the Hilbert space  $h^{-1}H = H$ . Thus,

$$d^2(I^{(0)} \circ h, I^{(1)} \circ h) = \inf_g \left\| I^{(0)} - I^{(1)} \circ (h \circ g \circ h^{-1}) \right\|_H^2 \quad (26)$$

$$= \inf_{g' = h \circ g \circ h^{-1}} \left\| I^{(0)} - I^{(1)} \circ g' \right\|_H^2 = d^2(I^{(0)}, I^{(1)}). \quad (27)$$

The metric property consists of a check of symmetry and triangular inequality properties.  $\square$

Properties of the metric distance  $d(I^{(0)}, I^{(1)})$  allow an efficient alternating minimization algorithm for the optimization problem given by Lemma 2. In fact, (18) implies that flow  $J_t = I_t \circ g_t^{-1}$  is also given as a linear combination of its boundary conditions

$$J_t = (1-t) \left( I^{(0)} \circ g_t^{-1} \right) + t \left( I^{(1)} \circ (g_t^{-1} \circ g_1) \right). \quad (28)$$

On the other hand, with  $J_t$  fixed, velocities  $\Omega(t)$  and  $\beta(t)$  are given as the solution of a simple quadratic optimization problem

$$(\Omega(t), \beta(t)) = \arg \inf_{\Omega(t), \beta(t)} \int_0^1 \left\| \frac{\partial J_t}{\partial t} + \left\langle \frac{\partial J_t}{\partial x}, \Omega(t)x + \beta(t) \right\rangle_{\mathbb{R}^k} \right\|_H^2 dt. \quad (29)$$

Thus, both the minima in  $J_t$  and  $\Omega(t), \beta(t)$  with, respectively,  $\Omega(t), \beta(t)$  and  $J_t$  fixed, are given by closed-form expressions. This suggests the following alternating minimization algorithm for computing  $d(I^{(0)}, I^{(1)})$ . Starting with  $g_t^{(0)} = id$  and  $J_t^{(0)} = (1-t)I^{(0)} + tI^{(1)}$ , we apply the following iterative scheme:

1.

$$\left( \Omega^{(n+1)}(t), \beta^{(n+1)}(t) \right) = \arg \inf_{\Omega(t), \beta(t)} \int_0^1 \left\| \frac{\partial J_t^{(n)}}{\partial t} + \left\langle \frac{\partial J_t^{(n)}}{\partial x}, \Omega(t)x + \beta(t) \right\rangle_{\mathbb{R}^k} \right\|_H^2 dt.$$

2.  $g_t^{(n+1)} = (R^{(n+1)}(t), b^{(n+1)}(t))$ , where

$$R^{(n+1)}(t) = \int_0^t \exp\left(\Omega^{(n+1)}(\sigma)\right) d\sigma,$$

$$b^{(n+1)}(t) = \int_0^t \left[ R^{(n+1)}(t) - R^{(n+1)}(\sigma) \right] \beta^{(n+1)}(\sigma) d\sigma.$$

3.

$$J_t^{(n+1)} = (1-t)I^{(0)} \circ \left( g_t^{(n+1)} \right)^{-1} + t \left( I^{(1)} \circ g_1^{(n+1)} \right) \circ \left( g_t^{(n+1)} \right)^{-1}.$$

The iterative process is expected to converge to the values of  $J_t$ ,  $\Omega(t)$ , and  $\beta(t)$  which attain the infimum for  $d(I^{(0)}, I^{(1)})$ . Fig. 1 displays the minimum energy path  $J_t$  connecting an image  $I^{(0)}$  of a tank in trees to its template  $I^{(1)}$ .

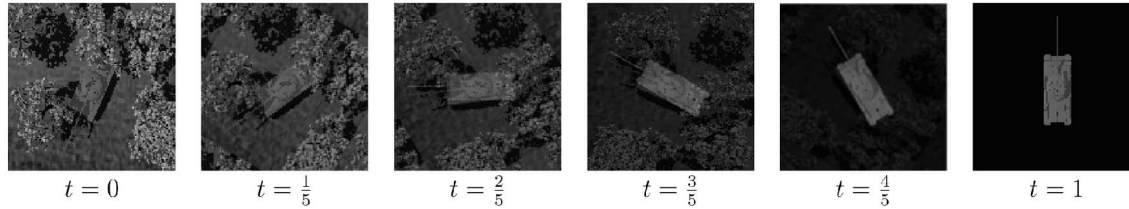


Fig. 1. Path  $J_t$  connecting  $I^{(0)}$  (panel 1) to  $I^{(1)}$  (panel 6) at times  $t = 0, \frac{1}{5}, \dots, 1$ .

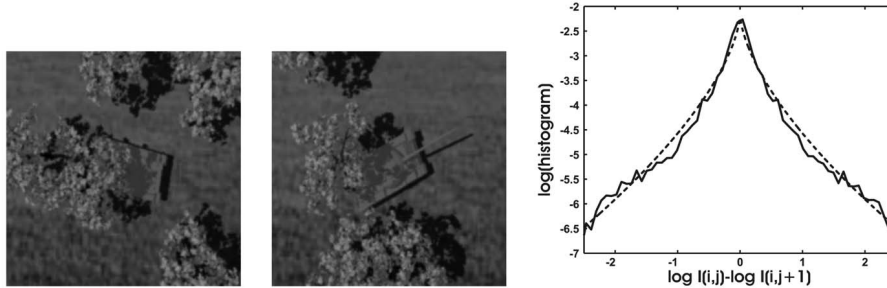


Fig. 2. Panels 1-2 show synthesized target chips. Panel 3 shows derivative statistics for synthetic clutter images. Solid curve—observed; dashed—generalized Laplace distribution  $(\alpha, s) = (0.637, 0.254)$ .

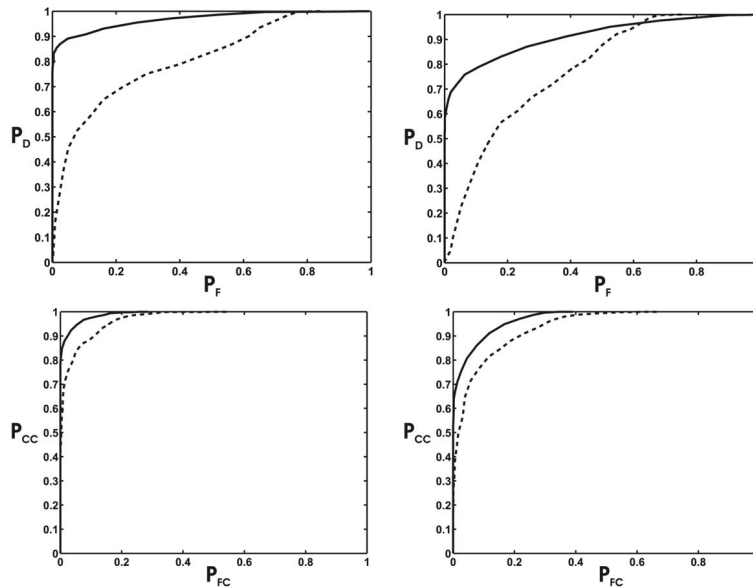


Fig. 3. Top row displays ROC curves for detection of a T72 tank for low density (left panel) and high density (right panel) of clutter; solid line—covariance norm; dashed line—Euclidean norm. Bottom row shows ROC curves for target identification in low (left panel) and high (right panel) clutter densities; solid line—covariance norm; dashed line—Euclidean norm.

### 3 TARGET DETECTION/IDENTIFICATION IN EO IMAGERY

This section presents numerical results on target detection/identification in optical images of targets in clutter. For the numerical experiments presented below, we synthesized a data set of target chips in natural clutter using 3D ray-tracing rendering. The re-rendered images in the data set contain targets in randomly synthesized terrain taking into account occlusion, shadows and lighting variation as well as other effects usually encountered in natural scenes. Fig. 2 displays example images from the synthetic data set. Such a process generates imagery which is extremely photo-realistic as exhibited by the fact that the statistics of the ray-traced images are non-Gaussian and follow the various powerlaws (see [9] for details). Working with the log intensities, we computed the marginal distribution of horizontal derivatives  $D = \ln I(i, j) - \ln I(i, j + 1)$ . Fig. 2 shows the logarithm

of the histogram of  $D$ . The histogram has a sharp peak at 0 and heavy tails. In [9], the density function  $f(x)$  of  $D$  is modeled as a generalized Laplace distribution  $f(x) = \frac{1}{2} \cdot e^{-|\frac{x}{s}|^\alpha}$ . The dashed curve in panel 3 of Fig. 2 presents the Laplace model of Mumford with the parameters  $(\alpha, s) = (0.637, 0.254)$  fitted to the empirical histogram of our data set.

In a statistical framework, target detection is formulated as a hypothesis testing problem and tackled using classic detection theory [12]. Assume a binary scenario with two hypotheses  $H_0$  and  $H_1$ , where, under the hypothesis  $H_0$ , the observed image contains no targets,  $I_D = W$ , and, under  $H_1$ , the target is present,  $I_D = I_{temp} \circ g + W$ . Note that the pose  $g$  is unknown and plays the role of a nuisance parameter. Generalized likelihood ratio test yields the following decision rule

$$d^2(I_D, 0) - d^2(I_D, I_{temp}) = \inf_{g \in G} \left\| \begin{matrix} H_1 \\ I_D - I_{temp} \circ g \\ H_0 \end{matrix} \right\|_H^2 > \nu. \quad (30)$$

The probability of correct detection  $P_D$  and the probability of a false alarm are given by  $P_D = \mathcal{P}[H_1|H_1]$  and  $P_F = \mathcal{P}[H_1|H_0]$ .

Similarly, the decision rule for target identification involves comparing metric distances from the observed image  $I_D$  to the corresponding target templates  $I^{(0)}$  (a jeep vehicle) and  $I^{(1)}$  (a T72 tank) under the hypotheses  $H_0$  and  $H_1$

$$d^2(I_D, I^{(0)}) - d^2(I_D, I^{(1)}) > \nu. \quad (31)$$

The probability of correct classification  $P_{CC}$  and the probability of false classification  $P_{FC}$  are given by  $P_{CC} = \mathcal{P}[H_1|H_1]$  and  $P_{FC} = \mathcal{P}[H_1|H_0]$ .

For each of the classes corresponding to the hypotheses  $H_0$  and  $H_1$ , we have randomly generated 1,000 target or clutter chips. The performance of the metric distance  $d(I^{(0)}, I^{(1)})$  was evaluated at two different values of the clutter density which is defined as the number of trees per unit area. The covariance of clutter was estimated from a large data set of synthetic images generated by the procedure described in the beginning of this section. The data set included image chips at different clutter densities, and the same single covariance was used for all the experiments presented below. Although neither real-world clutter images nor the synthesized ones are statistically stationary, the complexity can be reduced by using a cyclo-stationary model while still capturing important spatial statistical information. Under the cyclo-stationarity assumption, the clutter covariance is Toeplitz and its eigen basis  $\{\psi_n(x)\}$  is a Fourier basis. The corresponding eigenvalues  $\{\lambda_n\}$  were computed using classical spectrum estimation methods. Fig. 3 displays ROC curves for different clutter densities corresponding to the covariance norm  $\|\cdot\|_H$  and the Euclidean norm  $\|\cdot\|$  used here as the baseline. For both target detection and identification, the metric distance based on the second-order statistics of clutter significantly outperforms the Euclidean distance.

## 4 CONCLUSION

Using a differential-geometric approach, we have introduced a new metric distance for automated target recognition which reflects the statistics of clutter present in the observed imagery. The derived metric is invariant with respect to the pose of target and is robust to the infinite variety of natural clutter. While this metric is based on the second-order statistics of natural clutter, it significantly improves detection/identification rates. We should expect that a change in this metric would be appropriate for the non-Gaussian statistics that are being quantified in the community at this time.

## ACKNOWLEDGMENTS

This work was supported by the Office of Naval Research (ONR N00014-00-1-0327) and the Army Research Office (ARO DAAD19-99-1-0012 and ARO DAAD19-01-10644). The authors thank the anonymous reviewers for their helpful comments, which have improved the quality of this paper.

## REFERENCES

- [1] A. Yuille, "Deformable Templates for Face Recognition," *J. Cognitive Neuroscience*, vol. 3, no. 1, 1991.
- [2] M. Cooper and M. Miller, "Information Measures for Object Recognition Accommodating Signature Variability," *IEEE Trans. Information Theory*, vol. 46, no. 5, pp. 1896-1906, 2000.
- [3] P.N. Belhumeur, J. Hespanha, and D.J. Kriegman, "Eigenfaces vs. Fisherfaces: Recognition Using Class Specific Linear Projection," *Proc. European Conf. Computer Vision*, pp. 45-58, 1996.
- [4] M. Miller and L. Younes, "Group Actions, Homeomorphisms, and Matching: A General Framework," *Int'l J. Computer Vision*, vol. 41, no. 1/2, pp. 61-84, 2001.
- [5] S.C. Zhu, Y.N. Wu, and D. Mumford, "Filters, Random Field and Maximum Entropy (FRAME): Towards a Unified Theory for Texture Modeling," *Int'l J. Computer Vision*, vol. 27, no. 2, pp. 107-126, 1998.
- [6] G. Cross and A. Jain, "Markov Random Field Texture Models," *IEEE Trans. Pattern Analysis and Machine Intelligence*, vol. 5, no. 1, pp. 25-39, Jan. 1983.
- [7] R. Chellappa, "Two-Dimensional Discrete Gaussian Markov Random Field Models for Image Processing," *Pattern Recognition*, vol. 2, pp. 79-112, 1985.
- [8] U. Grenander and A. Srivastava, "Probability Models for Clutter in Natural Images," *IEEE Trans. Pattern Analysis and Machine Intelligence*, vol. 23, no. 4, pp. 424-429, Apr. 2001.
- [9] J. Huang and D. Mumford, "Statistics of Natural Images and Models," *IEEE Conf. Computer Vision and Pattern Recognition*, pp. 541-547, 1999.
- [10] L. Scharf and B. Friedlander, "Matched Subspace Detectors," *IEEE Trans. Information Theory*, vol. 42, no. 8, pp. 2146-2157, 1994.
- [11] E. Kelly, "An Adaptive Detection Algorithm," *IEEE Trans. Aerospace and Electronic Systems*, vol. AES-22, pp. 115-127, 1986.
- [12] H.L. van Trees, *Detection, Estimation, and Modulation Theory: Part I*. New York: John Wiley and Sons, 1968.

► For more information on this or any other computing topic, please visit our Digital Library at [www.computer.org/publications/dlib](http://www.computer.org/publications/dlib).